Three-dimensional imaging in degraded visual field

Three-dimensional imaging in degraded visual field

A. Oran[1], S. Ozharar[2] and I. Ozdur[3],

[1]*Abdullah Gül University, Kayseri, Turkey,*
[2]*Bahçeşehir University, Istanbul, Turkey,*
[3]*Abdullah Gül University, Kayseri, Turkey,*

E-mail: *abdullah.oran@agu.edu.tr*

Abstract. Imaging at degraded visual environments is one of the biggest challenges in today's imaging technologies. Especially military and commercial rotary wing aviation is suffering from impaired visual field in sandy, dusty, marine and snowy environments. For example during landing the rotor churns up the particles and creates dense clouds of highly scattering medium, which limits the vision of the pilot and may result in an uncontrolled landing. The vision in such environments is limited because of the high ratio of scattered photons over the ballistic photons which have the image information. We propose to use optical spatial filtering (OSF) method in order to eliminate the scattered photons and only collect the ballistic photons at the receiver. OSF is widely used in microscopy, to the best of our knowledge this will be the first application of OSF for macroscopic imaging. Our experimental results show that most of the scattered photons are eliminated using the spatial filtering in a highly scattering impaired visual field. The results are compared with a standard broad area photo detector which shows the effectiveness of spatial filtering.

1. Introduction, state-of-the-art, objectives and overview of the action

One of the biggest challenges in today's imaging technology is three-dimensional (3-D) imaging in degraded visual fields (DVF). Especially military and commercial rotary wing aviation is suffering from degraded visual environments in sandy, dusty, marine and snowy environments. In critical mission phases such as take-off and landing accidents are caused by reducing visibilities to near zero due to brownout, whiteout or water spray conditions from obscurant clouds created by the downwash of the rotor blades. Not only in landing but also in flying scenarios heavy fog and snow can easily impair the vision of the pilot. Some examples of degraded visual environments are shown in Figure 1.

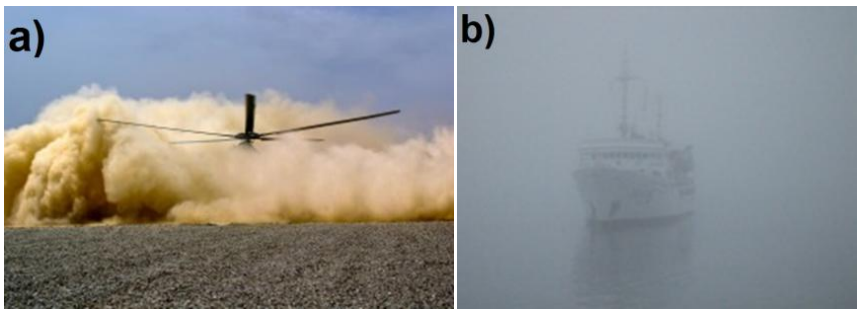

Figure 1. Examples of degraded visual environments: rotary wing brown out (Credit: revistaaerea.com) (a), fog in a marine environment (Credit: NOAA) (b).

This vision impairment in rotary wing aviation is resulted in many accidents and life losses in different countries. For example, the UK experienced 24 accidents in the 5 year period of 2005-2009, France has experienced 8 brownout mishaps in the past 15 years, German defense forces has experienced more than 30 mishaps in association with dust or snow. US department of defense report 60 crew members have lost their lives since 1990 due to the visual impairments in degraded visual environments. Many other countries (Canada, Sweden, Norway, and Netherlands) are also report losses and mishap due the degraded visual environments [1].

Degraded visual environments do not only effects rotary wind aviation; people are also affected by fog and snow in daily life especially while driving. According to a report prepared in US, in a 10 year average (2002-2012), 11,812 people are injured, 511 people are dead in 31,385 crashes *annually* in US [2].

One of the notable accidents due to fog was a maritime disaster occurred in 1956, a collision of the ocean liners the SS Andrea Doria and MS Stockholm. As a consequence of the collision 46 people died and SS Andrea Doria capsized and sank [3]. Heavy fog related some other notable accidents are the 1945 crash of a B-25 Mitchell into the Empire State Building [4] and the 1977 collision of Pam Am and KLM planes at the Tenerife Airport [5].

Degraded visual environments are also a problem for subsea investigations. Even for very short distances (a few meters) the visibility can be very poor [6]. These aforementioned cases are main motivations for developing systems to improve the eyesight of pilots, drivers, search and rescue teams, and firefighter

There are mainly 3 different sensor technologies that offer potential solutions to imaging at degraded visual environments; these technologies are based on RADAR, LIDAR and passive sensors.

RADAR related technologies are based on dust penetration capabilities of mm wave signals (35-95 GHz). Their current limitation is low resolution due to the relatively long wavelength. Because of the strong demand from avionics industry there are commercial products based on this technology, however the research is still going on for better resolution and longer ranges [7]–[9]. The second sensor technology is LIDAR based 3D sensors. These sensors transmit an optical pulse to the area that will be imaged and then detects the reflected optical pulse with fast electronics. When compared with RADAR based sensors, LIDAR based 3D sensor have potential to offer higher resolution and there are promising products from different vendors [10], [11]. The third and the last sensor technology is the passive sensors. Passive sensors rely on thermal imaging but operating at longer wavelengths. Current technologies operate at 94 GHz and exploit naturally reflected and emitted radiation [12].

The LIDAR systems are especially common in 3-D applications such as forest management and planning, flood modeling, determining structural characteristic of land [13] and the Google self-driving car [14]. It can receive an image with high spatial resolution and accuracy remotely; it can detect both ballistic and scattering photons as well. Since; there is no problem of reaching saturation similar with a detector. However; in DVF, the scattering photons may become dominant over the ballistic photons and prevent original image because the LIDAR cannot distinguish the difference between the ballistic and scattering photons. Herein, this paper presents a method of improving the imaging capabilities in degraded visual environments using a *LIDAR based 3D sensor*. In order to achieve this, we investigated the *optical spatial filtering (OSF)* properties for *coherent* 3D LIDAR architectures.

2. Research methodology and approach

Imaging through degraded visual environments is a very challenging problem and research and development is still going on. Our approach on the problem is 3D coherent LIDAR technology with optical spatial filtering. Optical spatial filtering is a technique in which a lens focuses an image/beam to a pinhole. In this technique only the beams with the correct wavefront can pass through the pinhole.

Any disturbances on the wavefront will be filtered. One of the main applications of the pinholes is cleaning up laser beams from any unwanted intensity variations [15], Figure 2a. Another application of optical spatial filtering is to filter out the out-of-focus light. This property is used in confocal

microscopy where a laser beam is focused to a focal plane and then a lens and pinhole pair is used to collect light *only from the focal plane* [16], Figure 2*b*. The wavefront coming from out-of-focus does not have the correct wavefront for the light to pass through the pin hole.

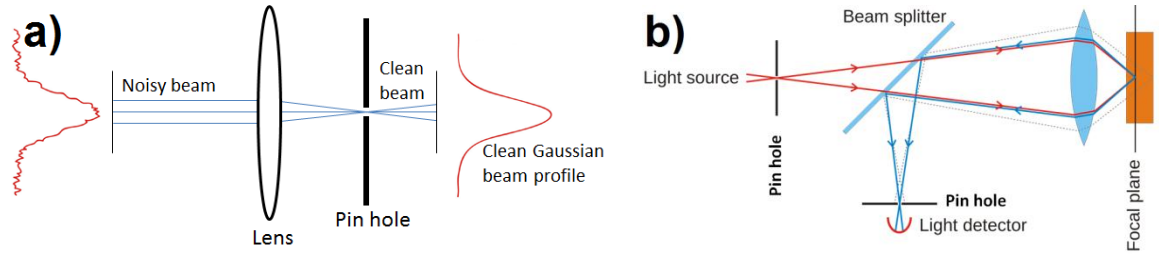

Figure 2. Application of pin holes: cleaning up Gaussian beams (a) and collecting light only from the focal plane (b).

In this paper, the intensity noise and out-of-focal light filtering effect was used in order to filter out the scattering light from the receiver.

In a typical 3D imaging LIDAR system, the signal-to-noise ratio is limited by the amount of collected light. In these systems the link loss can be as high as 100 dB, so the amount of receiver optical power is very small and the noise floor is limited by the shot noise or noise of sub-components [17]. In order to increase the amount of collected beam, broad area detectors and multimode fibers are used at the receiver. At degraded visual environments the signal-to-noise ratio (SNR) is not limited by the amount of collected light or sub-components but it is limited by the scattered light, that's why increasing the collection efficiency in such systems does not help to solve the problem. In order to eliminate the scattered light we used optical spatial filtering at degraded visual environments.

In the experimental setup, shown in Figure 3, an ultra-narrow linewidth (< 1 kHz) laser, working at 1550 nm is used as the light source. An isolator is placed after the laser in order to eliminate any unwanted back reflections. A power splitter is used to measure the power of the laser. The laser beam is sent to the DVF medium using a free space coupler and survived light beams from DVF are measured by different detectors at the back of the DVF medium.

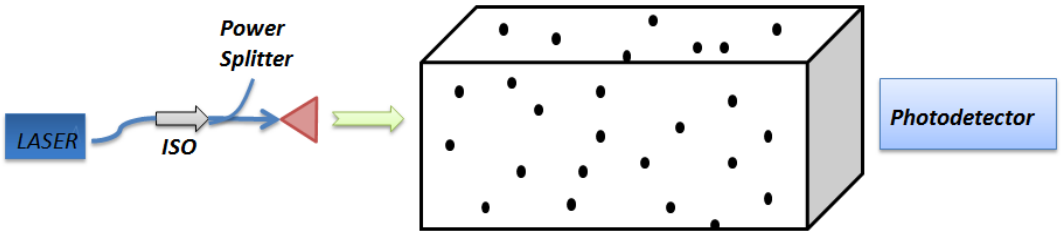

Figure 3. Experimental setup (iso: isolator).

The experiments were done in a homemade degraded visual environment. Cement powder is used to create a DVF effect, and particle size distribution of the powder is given in Figure 4. The experiments were repeated on two separate occasions when the tank is empty and filled with the cement material in order to measure the effectiveness of the optical spatial filtering.

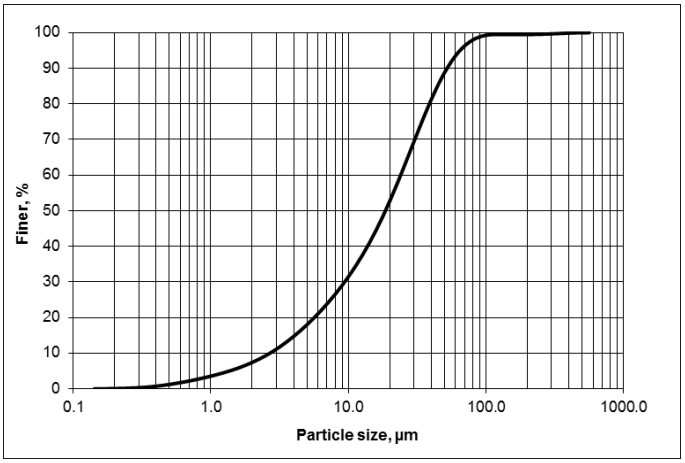

Figure 4. Particle size of cement used in the experiment.

In a degraded visual environment there are two photon types to deal with, the scattering photons and the ballistic photons. The scattering photons reach to the detector after bouncing many times from the particles in the environment. Whereas the ballistic photons arrive directly to the detector without experiencing any scattering. A broad area (or multimode) receiver does not distinguish the scattering and ballistic photons and collect all of them. In Figure 5, the receiver architecture with a broad area detector is shown. In this setup, all the photons coming from the degraded visual environments, including scattering photon 1 and 2 are detected by the detector which is not desirable for high SNR.

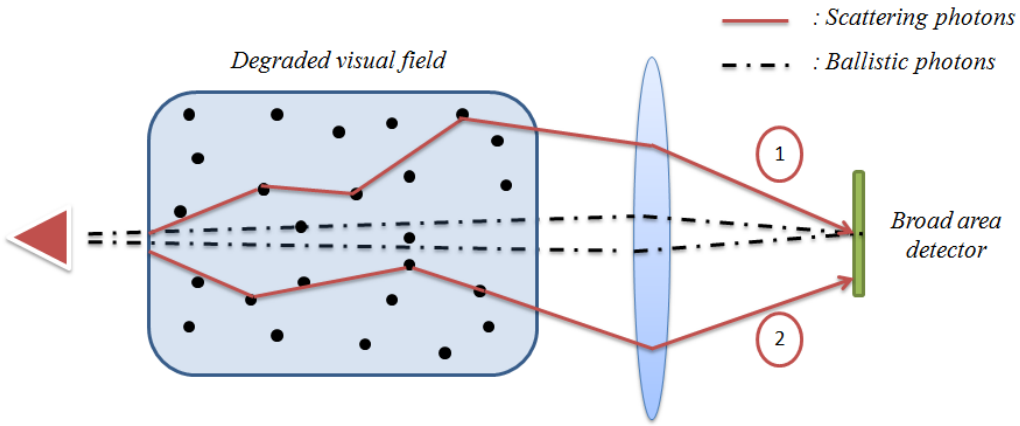

Figure 5. Receiver architecture with broad area detector (the size is exaggerated) for visual aid.

When the tank is empty and using broad area detector, all the detected photons are ballistic photons and there are no scattering photons. The distribution of the ballistic photons can be seen in Figure 6 black curve, in this figure the x-axis is the distance from the on axis. If the medium is filled with particles then both the ballistic and scattered photons are present at the detection plane. The distribution of the ballistic and scattered photons can be seen in Figure 6 red curve. As expected the collected photons have a broader distribution from the former case which is a result of broad area detection.

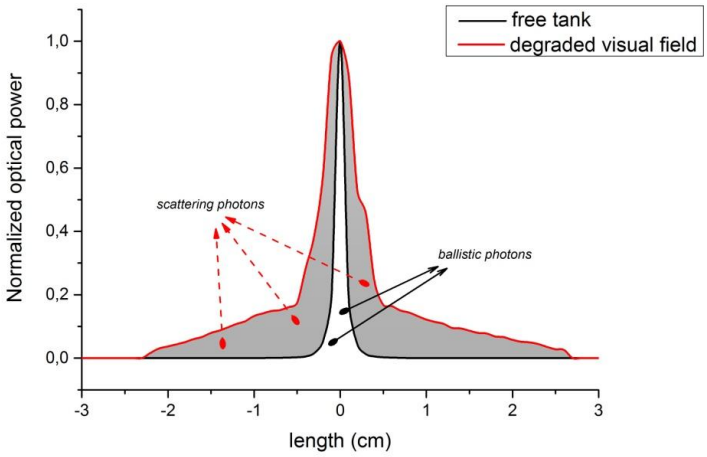

Figure 6. Optical power of broad area detector for two cases: free tank and DVF.

To eliminate effects of scattering photons, another architecture is prepared, shown in Figure 7. The transmitted beam is shown with blue lines. If the transceiver system is focused on the target (as shown in the Figure 7) only the light that is coming from the path of the beam will be coupled back to the fiber in other words out-of-focus light filtering will be achieved. In coherent LIDAR transceiver architecture less photons are coupled back to the fiber that is why it is not preferable in 3D LIDAR systems. However for 3D imaging at degraded visual environment systems the signal-to-noise ratio of the system is not limited by the amount of light coupled back to the fiber but it is limited by the ratio of scattering photons.

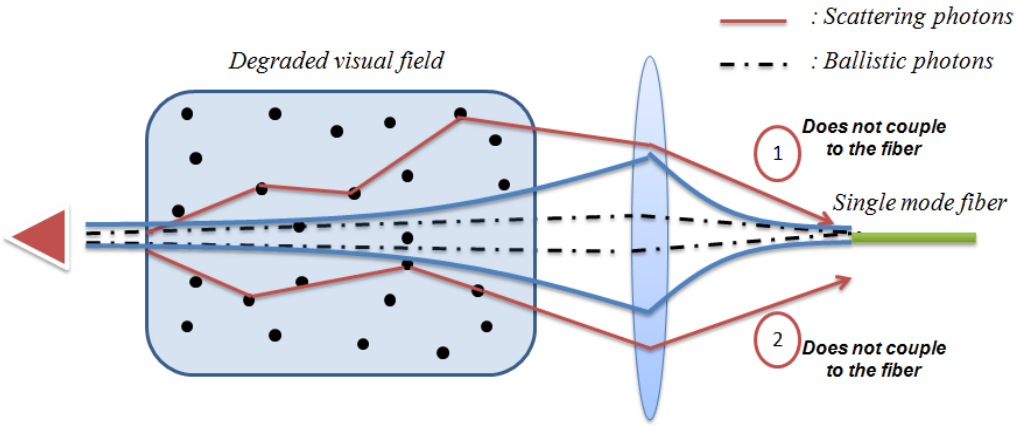

Figure 7. Receiver architecture with single mode fiber.

In this architecture the scattered light is less likely to couple to the fiber. For example the scattered photon 1 does not couple to the fiber even though it falls on the fiber as it does not have the right $\vec{k}$ vector (or the incoming angle is bigger than the acceptance angle) and photon 2 does not couple to the fiber simply because it does not fall on the fiber. The ballistic beams on the other hand come directly to the fiber and can easily couple to the fiber. In this setup the detected number of ballistic photons are not changing however detected scattered photon number decreases significantly, which will result in a better signal-to-noise ratio. Measured optical power is plotted for different off axis distances in Figure 8. From the figure we observe that most of the scattering photons are eliminated by optical spatial filtering method.

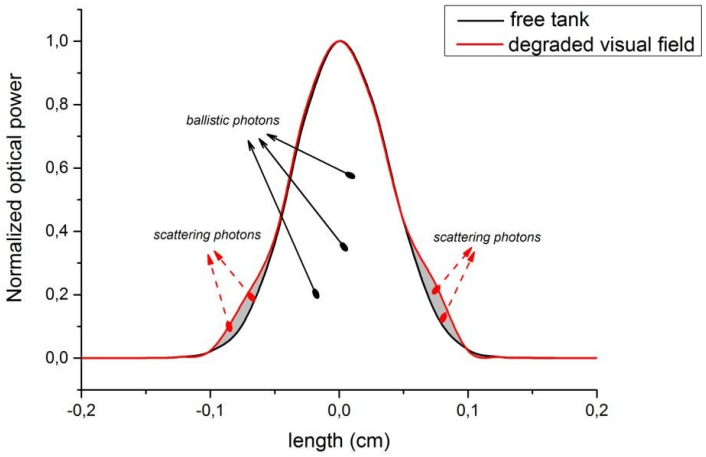

Figure 8. Optical power of SMF for two cases: free tank and DVF.

3. System Comparison

3.1. Error Results:

The relative error is defined as the ratio of the absolute error, which is defined as the magnitude of the difference between the DVF and the free tank over the magnitude of the ballistic photons. According to values of two Figures (3 and 6); error rate are respectively 0.830 and 0.056.

3.2. Correlation Results:

All two architecture systems and two cases were simulated and compared based on a projected reach. However, for highest confidence we analyzed two performance comparisons with MATLAB.

Tablo 1. Significant coefficients of two system performances.

	BAD: free tank	BAD: DVF	SMF: free tank	SMF: DVF
BAD: free tank	1	0.676 0.000	x	x
BAD: DVF	x	1	x	x
SMF: free tank	x	x	1	0.997 0.000
SMF: DVF	x	x	x	1

According to the Table 1, there are two hypotheses that can be made comparison for **BAD: free tank** *(data 01)* ~ **BAD: DVF** *(data 02);*

- H_0: There is no significant correlation between the *data 01* and *data 02.*
- H_1: There is a significant correlation between the *data 01* and *data 02.*

The returned value of significant = 0,000<0,05 indicates that H_0 hypothesis is rejected . As a result, there is a significance correlation statistically between *data 01* and *data 02* at the % 95 confidence interval as represented in the equation below:

$$\square_{data01,data02}=0.676 \quad (1)$$

For second performance of our system is compared same idea; **SMF: free tank** *(data 03)* ~ **SMF: DVF** *(data 04).*

- H_0: There is no significance correlation between the *data 03* and *data 04.*
- H_1: There is a significance correlation between the *data 03* and *data 04*.

The returned value of significant= 0,000<0,05 indicates that H_0 hypothesis is rejected . As a result, there is a significance correlation statistically between *data 03* and *data 04* at the 95% confidence interval as represented in the equation below:

$$\square_{data03,data04}=0.997 \quad (2)$$

3.3. T-Test Results:

Tablo 2. Distributions of two comparisons.

	Mean	Variance
BAD: free tank	39700.5701	7.292e-10
BAD: DVF	5.3533	124.335
SMF: free tank	273938.7574	2.694e-11
SMF: DVF	292.5565	280416.89

Hypothesis test result is returned as a logical value. H=ttest2(x,y) performs a t-test of the hypothesis that two independent samples, in the vectors *BAD: DVF* and *SMF: DVF* (from Table 2) represented as x and y , come from distributions with equal means, and returns the result of the test in h.

- If h = 1, this indicates the rejection of the null hypothesis (means $\mu_1 = \mu_2$) at the 5% significance level.
- If h = 0, this indicates a failure to reject the null hypothesis at the 5% significance level.

Test the null hypothesis that the pairwise difference between data vectors of **BAD: in case of DVF** and **SMF: in case of DVF** has a mean equal to zero;

```
[h,p] = ttest2(x,y)
>>h =1
>>p =   1.9197e-07
```
(3)

The returned value h=1 indicates that *ttest* rejects the null hypothesis at the default 5% significance level. That means, there is significance different statistically between the BAD: in case of DVF and SMF: in case of DVF at the 95% confidence interval.

4. Conclusions

In this work we used optical spatial filtering method in order to eliminate scattering photons for degraded visual fields. We compared two different detection schemes, one of them is a broad area

detector and the other one is a single mode fiber which will have optical spatial filtering effect. Our results show that using the optical spatial filtering effect the ratio of scattering photons are decreased to 5 % from 83 %. The filtering of scattering photons in a scattering medium will improve the imaging performance significantly.

This work is supported by TUBİTAK (The Scientific and Technological Research Council of Turkey) BİDEB Project number 113C029.

References

[1] R. T. O. T. Report, *Rotary-Wing Brownout Mitigation : Technologies and Training (Remèdes contre le phénomène de brownout*, vol. 323, no. January. 2012.
[2] Booz-Allen-Hamilton, "Ten-year averages from 2002 to 2012 based on nhtsa data," *US Dep. Transp. - Fed. Highw. Adm.*, 2012.
[3] Wikipedia, "SS Andrea Doria," 2016. [Online]. Available: https://en.wikipedia.org/wiki/SS_Andrea_Doria. [Accessed: 10-Feb-2016].
[4] Wikipedia, "B-25 Empire State Building crash," 2016. [Online]. Available: https://en.wikipedia.org/wiki/B-25_Empire_State_Building_crash. [Accessed: 10-Feb-2016].
[5] Wikipedia, "Tenerife airport disaster," 2016. [Online]. Available: https://en.wikipedia.org/wiki/Tenerife_airport_disaster. [Accessed: 10-Feb-2016].
[6] D. McLeod and J. Jacobson, "Autonomous Inspection using an Underwater 3D LiDAR," *... , San Diego Mar. ...*, 2013.
[7] J. Fritz, A. J. Gasiewski, and K. Zhang, "3D surface imaging through visual obscurants using a sub-THz radar," vol. 9087, p. 908702, 2014.
[8] B. Sykora, "BAE Systems Brownout landing aid system technology (BLAST) system overview and flight test results," pp. 1–15, 2009.
[9] R. D. Visual and E. Solution, "Enhanced Vision Solution for Degraded Visual Environment Enhanced Vision Solution for Degraded Visual Environment."
[10] E. Trickey, P. Church, and X. Cao, "Characterization of the OPAL obscurant penetrating LiDAR in various degraded visual environments," *Proc. SPIE*, vol. 8737, no. 613, p. 87370E–87370E–9, 2013.
[11] J. T. Murray, J. Seely, J. Plath, E. Gotfreson, J. Engel, B. Ryder, N. Van Lieu, R. Goodwin, T. Wagner, G. Fetzer, N. Kridler, C. Melancon, K. Panici, and A. Mitchell, "Dust-Penetrating (DUSPEN) 'see-through' lidar for helicopter situational awareness in DVE," vol. 8737, p. 87370H–87370H–8, 2013.
[12] T. E. Dillon, C. a. Schuetz, R. D. Martin, D. G. Mackrides, S. Shi, P. Yao, K. Shreve, C. Harrity, and D. W. Prather, "Passive, real-time millimeter wave imaging for degraded visual environment mitigation," vol. 9471, p. 947103, 2015.
[13] Wikipedia, "Lidar." [Online]. Available: https://en.wikipedia.org/wiki/Lidar. [Accessed: 10-Feb-2016].
[14] Wikipedia, "Google self-driving car." [Online]. Available: https://en.wikipedia.org/wiki/Google_self-driving_car. [Accessed: 10-Feb-2016].
[15] "Thorlabs.com - Precision Pinholes." [Online]. Available: http://www.thorlabs.de/NewGroupPage9_PF.cfm?Guide=10&Category_ID=22&ObjectGroup_ID=1400. [Accessed: 08-Feb-2016].
[16] K. Shi, P. Li, S. Yin, and Z. Liu, "Chromatic confocal microscopy using supercontinuum light," *Opt. Express*, vol. 12, no. 10, p. 2096, 2004.
[17] P. Toliver, I. Ozdur, A. Agarwal, and T. K. Woodward, "Comparison of LIDAR system performance for alternative single-mode receiver architectures: modeling and experimental validation," in *Proceedings of SPIE - The International Society for Optical Engineering*, 2013, vol. 8731, p. 87310W.